

Deuterium Kinetic Isotope Effects in the Gas-Phase S_N2 Reactions of Solvated Fluoride Ions with Methyl Halides[†]

Shuji Kato,^{*,‡} Jale Hacaloglu,[§] Gustavo E. Davico,^{||} Charles H. DePuy,[‡] and Veronica M. Bierbaum^{*,‡}

Department of Chemistry and Biochemistry, University of Colorado, Boulder, Colorado 80309-0215, Department of Chemistry, Middle East Technical University, 06531 Ankara, Turkey, and Department of Chemistry, University of Idaho, Moscow, Idaho 83844

Received: May 18, 2004; In Final Form: July 19, 2004

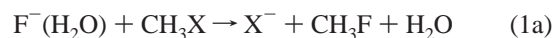
Rate constants and deuterium kinetic isotope effects (KIEs) are measured for gas-phase nucleophilic substitution (S_N2) reactions of solvated fluoride ions of $F^-(\text{methanol}) + \text{CH}_3\text{X}$ ($X = \text{Br}, \text{I}$), $F^-(\text{isopropyl alcohol}) + \text{CH}_3\text{I}$, and $F^-(\text{hydrogen fluoride}) + \text{CH}_3\text{I}$ at 300 K. The isotope effects are determined as the rate constant ratio k_H/k_D for specifically deuterated reactants, that is, methanol (CH_3OH , CD_3OH , CH_3OD , and CD_3OD), isopropyl alcohol ($i\text{-C}_3\text{H}_7\text{OH}$ and $i\text{-C}_3\text{H}_7\text{OD}$), hydrogen fluoride (HF and DF), and methyl halides (CH_3X and CD_3X). The data reveal identical trends to those previously observed for $F^-(\text{water}) + \text{CH}_3\text{X}$ (O'Hair, R. A. J.; Davico, G. E.; Hacaloglu, J.; Dang, T. T.; DePuy, C. H.; Bierbaum, V. M. *J. Am. Chem. Soc.* **1994**, *116*, 3609). The S_N2 reactivities decrease as reaction exothermicity decreases ($\text{CH}_3\text{I} > \text{CH}_3\text{Br} > \text{CH}_3\text{Cl}$) and as the nucleophile is solvated. Moderate inverse kinetic isotope effects ($k_H/k_D < 1$) are observed for the deuteration of the methyl halide, whereas substantial inverse KIEs are measured for the deuteration of the hydroxyl group of the solvent (or the deuteration of hydrogen fluoride). Moderate inverse KIEs are also measured for the deuteration of the methyl group in methanol. The observed trends and magnitudes of the isotope effects are rationalized qualitatively in terms of the S_N2 transition-state structure and bonding interactions analogous to those in the $F^-(\text{H}_2\text{O}) + \text{CH}_3\text{X}$ system.

Introduction

A considerable amount of study has addressed the structure, energetics, and reactivity of microsolvated cluster ions^{1,2} with the aim of understanding bulk solution chemistry from systematic gas-phase studies. Core ions (hydroxide, halides, etc.) are solvated with single or multiple molecules of water, alcohols, and other solvent species of organic and atmospheric interest. These cluster ions are allowed to react with neutral reagents, and the rate constants, isotope effects, and product distributions are determined as a function of the cluster size and composition.

Nucleophilic substitution (S_N2) is one of the most fundamental chemical transformations in solution and has been studied extensively in the field of gas-phase microsolvation chemistry.^{1,2} Solvated fluoride ions display facile reactivities, and the corresponding bare-ion data are also available. The reactions of microsolvated fluoride ions have thus been studied in some detail. Bohme and Raksit first examined the rate constants and products for the S_N2 reactions of the solvated fluoride ion: $F^-(\text{solvent})_{0-3} + \text{CH}_3\text{Cl}$, CH_3Br for D_2O , methanol, and ethanol as the solvent molecules.³ Seeley et al.⁴ used the temperature-variable selected-ion flow-tube technique to study $F^-(\text{H}_2\text{O})_{0-5} + \text{CH}_3\text{Br}$ reactions and refined some of the earlier kinetic data. In the reactions of $F^-(\text{H}_2\text{O})$ with methyl halides CH_3X , O'Hair et al. found the production of X^- to be the major channel (eq 1a), whereas the formation of $X^-(\text{H}_2\text{O})$ is minor (eq 1b) despite

the more favorable energetics.⁵ Tachikawa⁶ conducted direct ab initio dynamics calculations for $X = \text{Cl}$ and explained the observed product branching ratio; the formation of $\text{Cl}^-(\text{H}_2\text{O})$ is dynamically constrained and takes place nonsynchronously with the S_N2 transformation.



($X = \text{Cl}, \text{Br}, \text{I}$)

Deuterium kinetic isotope effects (KIEs) have been shown to be a sensitive probe for the structures of S_N2 transition states.⁷ O'Hair et al. also measured the KIE for the reactions of $F^-(\text{H}_2\text{O}) + \text{CH}_3\text{X}$ (eq 1).⁵ Upon deuteration of the methyl group of methyl halides (CD_3X), the rate constants for deuterated compounds (k_D) are found to be greater than those for nondeuterated compounds (k_H) such that $\text{KIE} \equiv k_H/k_D < 1$ (inverse secondary deuterium KIE). This is consistent with the conventional S_N2 reaction mechanism involving a tight transition state.⁷ In addition, a significant inverse KIE was observed for the deuteration of the water solvent (D_2O).⁵ Hu and Truhlar used transition-state theory to calculate the KIE values for $F^-(\text{H}_2\text{O}) + \text{CH}_3\text{Cl}$.⁸ The predicted isotope effects are in excellent agreement with those of the experiment. The S_N2 transition-state structure and vibrational modes were characterized by high-level molecular orbital calculations.⁸ At the transition state, a solvent water molecule is attached to the attacking nucleophile F^- via a hydrogen bond (Figure 1A). Factor analysis revealed the origin of the solvent isotope effect

[†] Part of the special issue "Tomas Baer Festschrift".

* Corresponding authors. E-mail: shuji.kato@colorado.edu (S.K.), veronica.bierbaum@colorado.edu (V.M.B.).

[‡] University of Colorado.

[§] Middle East Technical University.

^{||} University of Idaho.

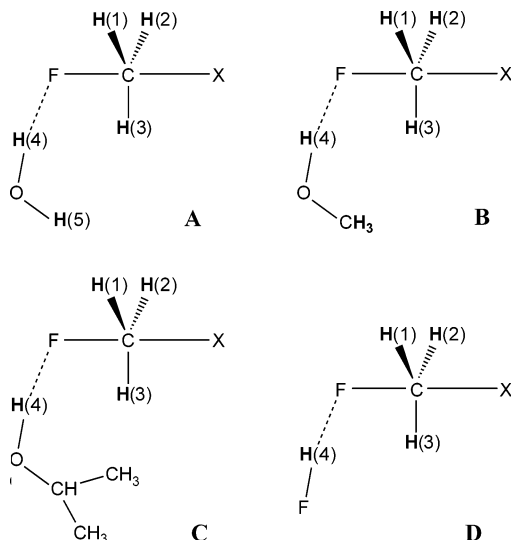


Figure 1. Schematic transition-state structures for S_N2 reactions of (A) $F^-(H_2O) + CH_3X$, (B) $F^-(CH_3OH) + CH_3X$, (C) $F^-(i-C_3H_7OH) + CH_3X$, and (D) $F^-(HF) + CH_3X$. Structures B–D are analogous to A, which has a reported theoretical structure.⁸ The bold font indicates hydrogen atoms that have been variously deuterated in these experiments.

as well as the conventional methyl halide KIE; the bent structure allows the remote water molecule to interact with the S_N2 center (and hence the reaction coordinate), thereby contributing to the inverse isotope effect observed.⁸

In the present paper, we extend the earlier study⁵ by investigating deuterium KIEs with different solvent molecules: $F^-(\text{methanol}) + CH_3Br$, $F^-(\text{methanol}) + CH_3I$, $F^-(\text{isopropyl alcohol}) + CH_3I$, and $F^-(\text{hydrogen fluoride}) + CH_3I$.⁹ The functional groups are individually labeled, that is, methanol (CH_3OH , CD_3OH , CH_3OD , and CD_3OD), isopropyl alcohol ($i-C_3H_7OH$ and $i-C_3H_7OD$), hydrogen fluoride (HF and DF), and methyl halides (CH_3X and CD_3X). Rate constants and KIEs are determined using the SIFT technique.¹⁰ The deuterium KIE is expected to give insights into the S_N2 transition state (or whether the reaction indeed proceeds via S_N2). Although no data are available for the transition state, the attacking nucleophiles have been characterized fairly well. Microwave spectroscopy indicates that $F^-(HF)$ is a linear structure ($D_{\infty h}$) with the F atoms attached symmetrically to hydrogen.¹¹ Theoretical calculations on $F^-(CH_3OH)$ and $F^-(i-C_3H_7OH)$ ¹² show that these species have similar structures to $F^-(H_2O)$,⁸ with the fluoride ion hydrogen bonded to the terminal hydroxyl group in an almost linear configuration. These results have led us to hypothesize that the S_N2 reactions could also proceed via transition-state structures (Figure 1B–D) that are similar to that for $F^-(H_2O) + CH_3X$. The measurement of deuterium KIEs would test this structure assignment as well as shed light on the dynamics of the ion–molecule reactions.¹³

Experimental Section

The experimental procedures are similar to those described previously^{5,10,14} and are outlined only briefly here. The reactions were carried out in a flowing afterglow-selected ion flow tube (FA-SIFT). The reactant ions were generated in the source flow tube by electron impact on nitrogen trifluoride to form F^- , which subsequently clusters with added solvent molecules. The reactant cluster ions were mass selected using a quadrupole mass filter and gently injected into the second flow tube where they were thermalized by collision with the He buffer gas (0.5 Torr, 300

K). Measured flow rates of methyl bromide or methyl iodide were added downstream through the manifold of inlets, and kinetic depletion of the reactant ions and the formation of reaction products were monitored using the detection quadrupole mass filter. Pairs of reactions involving deuterated and non-deuterated reactants were studied in back-to-back experiments on the same day under identical conditions. Absolute uncertainties in the measured rate constants are approximately $\pm 20\%$. However, systematic errors cancel in the rate constant ratio (k_H/k_D) so that the error bars in the KIE values are significantly smaller. (See below.) Methyl halides are obtained from commercial sources with nominal purities of 99.5% (CH_3Br and CH_3I) and 99.5% D (CD_3Br and CD_3I). Impurities in the reagents were further examined both by commercial analysis and by using the SIFT instrument as a chemical ionization assay,¹⁴ and it was confirmed that they have a negligible effect on the present results.

Results and Discussion

Rate Constants and KIEs. Table 1 summarizes the rate constants (k) and reaction efficiencies (k/k_{coll}) for the reactions of solvated fluoride ion with methyl bromide or iodide. The error bars associated with k represent one standard deviation of the mean of typically three measurements. The reaction efficiencies are defined as the ratio of the rate constants to the collision rate, which has been calculated using the parametrized trajectory collision rate theory.¹⁵ Electric dipole polarizabilities and permanent dipole moments are taken from Lide¹⁶ as $5.55 \times 10^{-24} \text{ cm}^3$ and 1.822 D (CH_3Br) and $7.97 \times 10^{-24} \text{ cm}^3$ and 1.62 D (CH_3I), respectively. The measured rates are generally smaller than those for the S_N2 reactions with bare F^- , by an order of magnitude for $F^-(\text{methanol}) + \text{methyl bromide}$ and a factor of roughly 3 for $F^-(\text{methanol}) + \text{methyl iodide}$. The reactions of methyl iodide with $F^-(\text{isopropyl alcohol})$ or $F^-(\text{hydrogen fluoride})$ are even slower. Because the values of the reaction efficiencies are well below unity (Table 1), it is expected that the small KIEs accurately reflect intrinsically small differences in the transition states of the deuterated and undeuterated reactants. In contrast for reactions that occur with high efficiency, that is, approach saturation, small differences in the transition states can be undetectable, and large differences in transition states can result in small KIEs.

The KIE values have been computed and grouped into three categories corresponding to the functional groups for deuteration (Table 1). The first column lists k_{CH_3X}/k_{CD_3X} , the rate constant ratio between nonlabeled and labeled methyl halides ($X = Br$ or I) for the same solvent with the same isotope composition (e.g., $F^-(CH_3OH) + CH_3Br$ vs $F^-(CH_3OH) + CD_3Br$). The second column is k_{CH_3}/k_{CD_3} , the rate constant ratio for the deuteration of the methyl group in methanol for the same methyl halide and with the same isotope composition elsewhere (e.g., $F^-(CH_3OH) + CH_3Br$ vs $F^-(CD_3OH) + CH_3Br$). The third column is k_{OH}/k_{OD} , the rate constant ratio for the deuteration of the hydroxyl group for the same methyl halide and with the same isotope composition elsewhere (e.g., $F^-(CH_3OH) + CH_3Br$ vs $F^-(CH_3OD) + CH_3Br$). In addition, the fourth column gives KIEs for the complete deuteration of methanol (k_{CH_3OH}/k_{CD_3OD}) for the same methyl halide with the same isotope composition. KIEs for the deuteration of hydrogen fluoride (HF vs DF) are also shown in the last column. Error bars reflect the propagation of stated errors in the rate constant; systematic uncertainties in rate measurement ($\pm 20\%$) cancel in the rate constant ratio and, hence, in KIEs. The measured KIE values are all less than unity, indicating that the isotope effects are inverse.

TABLE 1: Rate Constants, Reaction Efficiencies, and Kinetic Isotope Effects for S_N2 Reactions of Methyl Halides

| reaction | k (10^{-10} cm ³ s ⁻¹) ^a | k/k_{col} ^b | $k_{\text{CH}_3\text{X}}/k_{\text{CD}_3\text{X}}$ ^c | $k_{\text{CH}_3}/k_{\text{CD}_3}$ ^d | $k_{\text{OH}}/k_{\text{OD}}$ ^e | $k_{\text{CH}_3\text{OH}}/k_{\text{CD}_3\text{OD}}$ ^f | $k_{\text{HF}}/k_{\text{DF}}$ ^g |
|---|---|---------------------------------|--|--|--|--|--|
| F ⁻ + CH ₃ Br ^h | 18.8 ± 0.2 | 0.71 | | | | | |
| F ⁻ + CD ₃ Br ^h | 19.2 ± 0.4 | 0.73 | 0.98 ± 0.02 | | | | |
| F ⁻ (CH ₃ OH) + CH ₃ Br | 1.63 ± 0.04 | 0.09 | | | | | |
| F ⁻ (CH ₃ OH) + CD ₃ Br | 1.89 ± 0.01 | 0.10 | 0.86 ± 0.02 | | | | |
| F ⁻ (CD ₃ OH) + CH ₃ Br | 1.96 ± 0.05 | 0.11 | | 0.83 ± 0.03 | | | |
| F ⁻ (CD ₃ OH) + CD ₃ Br | 2.13 ± 0.07 | 0.12 | 0.92 ± 0.04 | 0.89 ± 0.03 | | | |
| F ⁻ (CH ₃ OD) + CH ₃ Br | 2.23 ± 0.03 | 0.12 | | | 0.73 ± 0.02 | | |
| F ⁻ (CH ₃ OD) + CD ₃ Br | 2.46 ± 0.03 | 0.14 | 0.91 ± 0.02 | | 0.77 ± 0.01 | | |
| F ⁻ (CD ₃ OD) + CH ₃ Br | 2.76 ± 0.02 | 0.16 | | 0.81 ± 0.01 | 0.71 ± 0.02 | 0.59 ± 0.02 | |
| F ⁻ (CD ₃ OD) + CD ₃ Br | 3.08 ± 0.04 | 0.17 | 0.90 ± 0.01 | 0.80 ± 0.01 | 0.69 ± 0.03 | 0.61 ± 0.02 | |
| F ⁻ + CH ₃ I ^h | 19.4 ± 0.2 | 0.77 | | | | | |
| F ⁻ + CD ₃ I ^h | 19.7 ± 0.4 | 0.78 | 0.98 ± 0.02 | | | | |
| F ⁻ (CH ₃ OH) + CH ₃ I | 5.20 ± 0.07 | 0.31 | | | | | |
| F ⁻ (CH ₃ OH) + CD ₃ I | 5.80 ± 0.09 | 0.34 | 0.90 ± 0.02 | | | | |
| F ⁻ (CD ₃ OH) + CH ₃ I | 5.78 ± 0.10 | 0.35 | | 0.90 ± 0.02 | | | |
| F ⁻ (CD ₃ OH) + CD ₃ I | 6.27 ± 0.05 | 0.38 | 0.92 ± 0.02 | 0.93 ± 0.02 | | | |
| F ⁻ (CH ₃ OD) + CH ₃ I | 5.94 ± 0.10 | 0.35 | | | 0.88 ± 0.02 | | |
| F ⁻ (CH ₃ OD) + CD ₃ I | 6.60 ± 0.11 | 0.39 | 0.90 ± 0.02 | | 0.88 ± 0.02 | | |
| F ⁻ (CD ₃ OD) + CH ₃ I | 6.86 ± 0.13 | 0.42 | | 0.87 ± 0.02 | 0.84 ± 0.02 | 0.76 ± 0.02 | |
| F ⁻ (CD ₃ OD) + CD ₃ I | 7.30 ± 0.13 | 0.44 | 0.94 ± 0.02 | 0.90 ± 0.02 | 0.86 ± 0.02 | 0.80 ± 0.02 | |
| F ⁻ ((CH ₃) ₂ CHOH) + CH ₃ I | 2.88 ± 0.05 | 0.18 | | | | | |
| F ⁻ ((CH ₃) ₂ CHOH) + CD ₃ I | 3.26 ± 0.06 | 0.20 | 0.88 ± 0.02 | | | | |
| F ⁻ ((CH ₃) ₂ CHOD) + CH ₃ I | 3.81 ± 0.03 | 0.24 | | | 0.76 ± 0.01 | | |
| F ⁻ ((CH ₃) ₂ CHOD) + CD ₃ I | 4.33 ± 0.03 | 0.27 | 0.88 ± 0.01 | | 0.75 ± 0.02 | | |
| F ⁻ (HF) + CH ₃ I | 0.0886 ± 0.0005 | 0.0047 | | | | | |
| F ⁻ (HF) + CD ₃ I | 0.113 ± 0.004 | 0.0060 | 0.78 ± 0.03 | | | | |
| F ⁻ (DF) + CH ₃ I | 0.150 ± 0.002 | 0.0081 | | | | | 0.59 ± 0.01 |
| F ⁻ (DF) + CD ₃ I | 0.183 ± 0.002 | 0.0099 | 0.82 ± 0.01 | | | | 0.62 ± 0.02 |

^a Error bars represent one standard deviation of the mean of three or more measurements. Absolute errors for k are approximately ±20%.

^b Reaction efficiency $\equiv k/k_{\text{col}}$, where the collision rate constant (k_{col}) is calculated using the parametrized trajectory collision rate theory.¹⁵ ^c Kinetic isotope effects for deuterium substitution on a methyl halide (X = Br or I). Error bars reflect the propagation of stated errors in the rate constants.

^d For deuterium substitution on the methyl group in methanol. ^e For deuterium substitution on the hydroxyl group in methanol or isopropyl alcohol.

^f For complete deuterium substitution on methanol. ^g For deuterium substitution on hydrogen fluoride. ^h Reference 5.

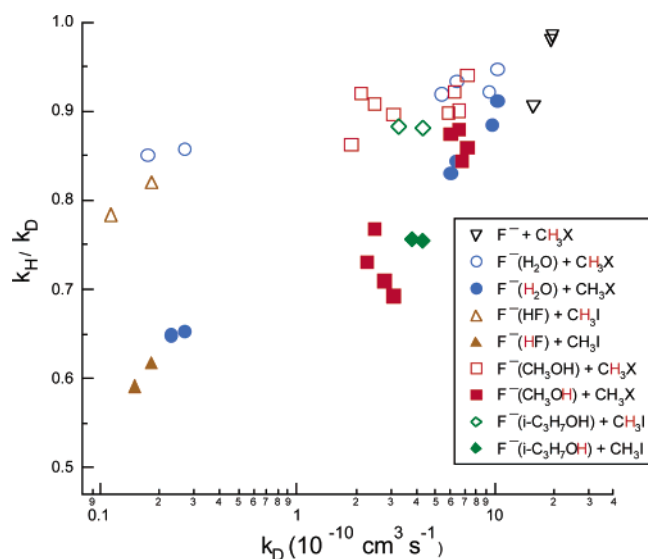


Figure 2. Kinetic isotope effects ($k_{\text{H}}/k_{\text{D}}$) plotted against the reaction rate constant (k_{D}). Open symbols represent the deuteration of methyl halides, whereas closed symbols represent the deuteration of the hydroxyl group (or of hydrogen fluoride). All data were taken from Table 1 except for F⁻ + CH₃Cl and F⁻(H₂O) + CH₃X (X = Cl, left four circles; X = Br, middle four circles; X = I, right four circles).⁵ The hydrogen sites that are pertinent to the isotope effect of concern are shown in red in the legend.

KIEs at the S_N2 Center Hydrogen Versus the Bridging Hydrogen. Figure 2 shows the deuterium KIEs ($\equiv k_{\text{H}}/k_{\text{D}}$) against the base rate constant k_{D} . Our previous results on F⁻ + CH₃X and F⁻(water) + CH₃X (X = Cl, Br, I) are also displayed.⁵ The S_N2 reactivities decrease as reaction exothermicity decreases (CH₃I > CH₃Br > CH₃Cl) and as the

nucleophile is solvated. Moderate inverse KIEs are observed for the deuteration of methyl halide (open symbols), whereas substantial inverse KIEs are observed for the deuteration of the bridging hydrogen (closed symbols). Both KIEs tend to approach unity as the rate constant becomes greater; reaction saturation may contribute slightly to the observed trend for rapid reaction systems of F⁻(H₂O) + CH₃Br, CH₃I and F⁻(CH₃OH) + CH₃I. Solvation with alcohol or hydrogen fluoride gives results that are entirely consistent with the trends that were previously observed for water solvation.⁵ This suggests that the S_N2 reactions proceed via a similar mechanism and that transition-state structures B–D in Figure 1 may be qualitatively valid. Essentially identical trends are observed when KIEs are plotted against reaction efficiencies (Table 1). It is noted that the values of KIEs “cluster” no matter how other parts of the system have been labeled. This implies that the KIEs are multiplicative, as previously noted for the case of F⁻(H₂O) + CH₃X.⁸ For example, the overall KIE for F⁻(CD₃OD) + CH₃Br ($k_{\text{CH}_3\text{OH}}/k_{\text{CD}_3\text{OD}} = 0.59$) is the product of the KIEs for F⁻(CD₃OH) + CH₃Br ($k_{\text{CH}_3}/k_{\text{CD}_3} = 0.83$) and F⁻(CH₃OD) + CH₃Br ($k_{\text{OH}}/k_{\text{OD}} = 0.73$). This fact further ensures that to a first-order approximation the observed kinetic isotope effects can be discussed separately for $k_{\text{CH}_3\text{X}}/k_{\text{CD}_3\text{X}}$, $k_{\text{CH}_3}/k_{\text{CD}_3}$, and $k_{\text{OH}}/k_{\text{OD}}$.

Despite the lack of knowledge on the detailed transition-state structures, energetics, and frequencies, the observed kinetic isotope effects $k_{\text{H}}/k_{\text{D}}$ can be qualitatively understood by analogy to the statistical treatment for F⁻(H₂O) + CH₃Cl.⁸

$$\text{KIE} = \eta_{\text{trans}} \eta_{\text{rot}} \eta_{\text{vib,low}} \eta_{\text{vib,mid}} \eta_{\text{vib,high}} \quad (2)$$

In this factor analysis, each η is the double ratio of partition functions. The partition function ratio between the transition

state and the reactants for H is divided by the corresponding ratio for D. Hu and Truhlar further factored the vibrational contribution into the following three components: high-frequency ($\nu_i > 2000 \text{ cm}^{-1}$), mid-frequency ($\nu_i = 600\text{--}2000 \text{ cm}^{-1}$), and low-frequency ($\nu_i < 600 \text{ cm}^{-1}$) modes (eq 2).⁸ They observed excellent agreement with the experimental inverse KIEs of O'Hair et al.⁵ This strongly suggests that the $\text{F}^-(\text{H}_2\text{O}) + \text{CH}_3\text{Cl}$ reaction proceeds statistically from reactants to the transition-state dividing surface.^{13,17} Although the unsolvated small $\text{S}_{\text{N}}2$ systems of F^- , $\text{Cl}^- + \text{CH}_3\text{Br}$ and F^- , Cl^- , $\text{Br}^- + \text{CH}_3\text{I}$ exhibit anomalous KIE trends¹⁴ that imply nonstatistical behavior, the systematic trends in Figure 2 suggest that the present large systems $\text{F}^-(\text{solvent}) + \text{CH}_3\text{X}$ behave statistically. We thus interpret the KIE results in terms of the partition function approach.

First, the deuteration of methyl halide is discussed. Hu and Truhlar found that the major factors responsible for the inverse KIE for $\text{F}^-(\text{H}_2\text{O}) + \text{CH}_3\text{Cl}$ are the low ($< 600 \text{ cm}^{-1}$)- and high ($> 2000 \text{ cm}^{-1}$)-frequency vibrational modes.⁸ The mid-frequency vibrational term is slightly greater than unity (normal) as is the translational term, whereas the rotational term is significantly greater than unity. However, it was later shown for the unsolvated reaction that the inverse $\eta_{\text{vib,low}}$ and normal translational and rotational contributions are an artifact because of the different number of degrees of freedom included in these groups for the reactants and the transition state, which is characteristic of bimolecular reactions.¹⁸ If these associated modes, which are rotational and translational modes in reactants that are converted into low-frequency modes in the transition state, are grouped together, then their contribution to the KIE is normal and nearly unity. Therefore, the significant terms become $\eta_{\text{vib,mid}}$ and $\eta_{\text{vib,high}}$, which are normal and inverse, respectively. However, the latter dominates, and the overall effect is that the KIE is inverse and dependent on the site of deuteration. At the $\text{S}_{\text{N}}2$ transition state for $\text{F}^-(\text{H}_2\text{O}) + \text{CH}_3\text{X}$ (Figure 1A) the out-of-plane C–H bending frequency ($\sim 1000 \text{ cm}^{-1}$) is lowered relative to that for the isolated reactant CH_3X ($\sim 1400 \text{ cm}^{-1}$), rendering $\eta_{\text{vib,mid}}$ slightly greater than unity (normal). As in the unsolvated reaction, this effect is overwhelmed by the strong inverse $\eta_{\text{vib,high}}$, and hence, the overall KIE is inverse.⁸ The C–H umbrella motion is considered to be largely unaffected by the remote ROH (R = H, CH_3 , $i\text{-C}_3\text{H}_7$) or HF groups (Figure 1), giving rise to relatively constant KIEs upon the deuteration of the methyl halides as observed (Figure 2). A large atom immediately adjacent to the attacking nucleophile atom sterically affects the C–H bending mode and modifies the KIE value.¹⁸ This crowdedness effect is likely to be negligible here because H(4) is the adjacent atom (Figure 1).

For the $\text{S}_{\text{N}}2$ reaction of $\text{F}^-(\text{H}_2\text{O}) + \text{CH}_3\text{Cl}$, the strong inverse $\eta_{\text{vib,high}}$ is primarily due to the stretching vibration between the oxygen atom and the hydrogen atom H(4) that is hydrogen bonded to fluorine.⁸ Hu and Truhlar used the MP2/aug-cc-pVDZ level of theory and showed that the O–H(4) frequency increases from 2261 cm^{-1} in isolated $(\text{HOH})\text{F}^-$ to 3124 cm^{-1} at the $[\text{HOH}(4)\cdots\text{F}-\text{CH}_3-\text{Cl}]^-$ transition state. The upward frequency change contributes to the inverse $\eta_{\text{vib,high}}$ when the hydroxyl group is deuterated. Physically, the frequency increase at the transition state is due to the partial charge transfer from F to CH_3Cl upon forming the transition state, thereby weakening the $\text{H}(4)\cdots\text{F}$ hydrogen-bonding interaction and thus strengthening the O–H(4) bond instead. In fact, the O–H stretching frequency at the transition state increases toward that for isolated H_2O ($\nu_1 = 3657 \text{ cm}^{-1}$, $\nu_3 = 3756 \text{ cm}^{-1}$).¹⁹ Hydrogen-bonding

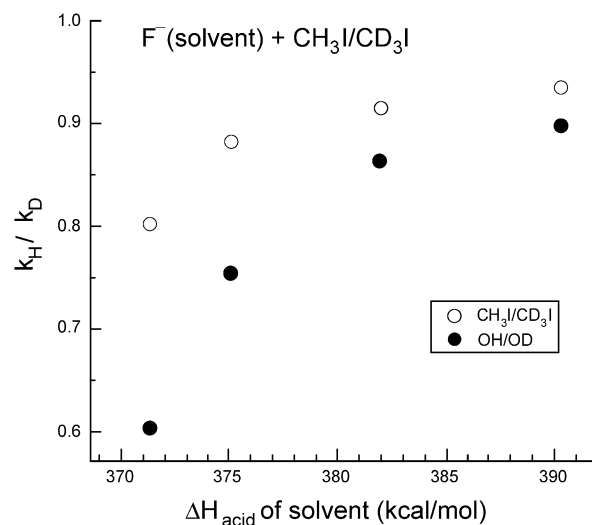


Figure 3. Kinetic isotope effects ($k_{\text{H}}/k_{\text{D}}$) plotted against the gas-phase deprotonation enthalpy of the solvent. The pairs of circles from left to right represent the solvents HF, $i\text{-C}_3\text{H}_7\text{OH}$, CH_3OH , and H_2O . Open circles indicate the deuteration of methyl iodide, whereas closed circles indicate the deuteration of the solvent hydroxyl group (or of hydrogen fluoride). Each data point is the average of KIEs for the applicable isotope variants (Table 1).

interactions for higher water clusters $\text{F}^-(\text{H}_2\text{O})_{1-6}$ have also been discussed computationally.²⁰

A similar mechanism is likely to be operative for the inverse KIEs that were observed upon the deuteration of the hydroxyl group in $\text{F}^-(\text{ROH})$ and also of hydrogen fluoride in $\text{F}^-(\text{HF})$. Bogdanov and McMahon predicted that the O–H stretching frequencies are 1968 and 2044 cm^{-1} for the $\text{F}^-(\text{CH}_3\text{OH})$ and $\text{F}^-(i\text{-C}_3\text{H}_7\text{OH})$ clusters, respectively, at the B3LYP/6-311++G(d,p) level of theory.¹² These frequencies are significantly lower than those for CH_3OH (3708 cm^{-1}) and $i\text{-C}_3\text{H}_7\text{OH}$ (3673 cm^{-1})¹² because of the $\text{H}\cdots\text{F}$ hydrogen bonds that formed. $\text{F}^-(\text{HF})$ is a linear structure with measured H–F stretching frequencies of 1286 cm^{-1} (ν_2) and 1336 cm^{-1} (ν_3),¹¹ significantly lower than the stretching frequency of 3962 cm^{-1} for diatomic hydrogen fluoride.²¹ Although no structure and vibrational data are available, it is very likely that the O–H (or F–H) frequency will increase at the $\text{S}_{\text{N}}2$ transition state. Strong inverse $\eta_{\text{vib,high}}$ will result upon the deuteration of the hydroxyl (or HF) group, as experimentally observed (Figure 2).

Hydrogen-bonding interactions in $\text{F}^-(\text{ROH})$ have been studied computationally.¹² If the acidity difference between ROH and HF decreases (e.g., $\Delta_{298}H_{\text{acid}}(\text{H}_2\text{O}) = 390.3 \text{ kcal mol}^{-1}$, $\Delta_{298}H_{\text{acid}}(\text{CH}_3\text{OH}) = 382.0 \text{ kcal mol}^{-1}$, and $\Delta_{298}H_{\text{acid}}(i\text{-C}_3\text{H}_7\text{OH}) = 375.1 \text{ kcal mol}^{-1}$ relative to $\Delta_{298}H_{\text{acid}}(\text{HF}) = 371.3 \text{ kcal mol}^{-1}$),²² then more charge transfer from F to ROH and, hence, a stronger $\text{ROH}\cdots\text{F}^-$ hydrogen bond would be expected. In fact, the measured exothermicity for association is greater for $\text{F}^- + i\text{-C}_3\text{H}_7\text{OH} \rightarrow \text{F}^-(i\text{-C}_3\text{H}_7\text{OH})$ ($33.5 \text{ kcal mol}^{-1}$)²³ than for $\text{F}^- + \text{CH}_3\text{OH} \rightarrow \text{F}^-(\text{CH}_3\text{OH})$ ($30.5 \text{ kcal mol}^{-1}$).¹² These values are between those for $\text{F}^-(\text{H}_2\text{O})$ ($27.4 \text{ kcal mol}^{-1}$)²⁴ and $\text{F}^-(\text{HF})$ ($45.7 \text{ kcal mol}^{-1}$).²² The stronger hydrogen bond in the free nucleophile may result in a more dramatic change (increase) in the O–H stretching frequency in going to the $\text{S}_{\text{N}}2$ transition state and, hence, result in a more inverse KIE. Figure 3 shows a correlation of the OH/OD (or HF/DF) KIE with the gas-phase deprotonation enthalpy of the solvent. The isotope effect for $\text{CH}_3\text{X}/\text{CD}_3\text{X}$ is also displayed for comparison. Upon the deuteration of the OH (or HF) group, stronger inverse KIEs are observed for nucleophiles with less acidity difference. This is consistent with the above dis-

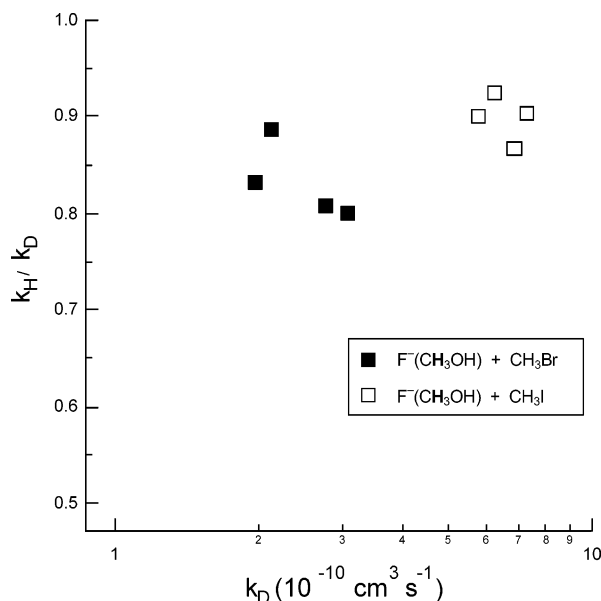


Figure 4. Kinetic isotope effects (k_H/k_D) for the deuteration of the methyl group in methanol plotted against the reaction rate constant (k_D). The hydrogen site pertinent to the isotope effect of concern is shown in bold font.

cussion. It has been suggested computationally,¹² however, that $i\text{-C}_3\text{H}_7\text{OH}\cdots\text{F}^-$ has a weaker hydrogen-bonding interaction than $\text{CH}_3\text{OH}\cdots\text{F}^-$, as indicated by the smaller decrease in the O–H stretching frequency (see above), the longer ROH \cdots F bond length (1.374 Å vs 1.339 Å), the lower H \cdots F stretching frequency (339 cm^{-1} vs 374 cm^{-1}), and the more localized charge on F (–0.884 vs –0.878). Clearly the hydrogen-bonding interaction is a complex issue; direct vibrational and structural data on the $\text{S}_{\text{N}}2$ transition state would be required to understand the KIE trend fully.

KIE at Methyl Group in Methanol. Figure 4 shows the KIE for the deuteration of the methyl group in the solvent methanol. The KIE values ($k_{\text{CH}_3}/k_{\text{CD}_3}$) are similar to those observed for the deuteration of the methyl halide ($k_{\text{CH}_3\text{X}}/k_{\text{CD}_3\text{X}}$). The origin of the inverse KIE is an intriguing issue for examination. Apparently, more remote from the $\text{S}_{\text{N}}2$ center (Figure 1B), the terminal CH_3 group may produce an isotope effect through a mechanism analogous to that for $\text{F}^-(\text{H}_2\text{O}) + \text{CH}_3\text{Cl}$.⁸ At the transition state for $\text{F}^-(\text{H}_2\text{O}) + \text{CH}_3\text{Cl}$ (Figure 1A), theory predicts that the terminal O–H(5) bending motion couples with the internal rotation of the CH_3Cl methyl group, giving rise to low-frequency fundamental modes ν_{18} (D_2O -sensitive) and ν_{19} (CD_3X -sensitive).⁸ These low-frequency modes ($<100 \text{ cm}^{-1}$) are nonexistent in the reactants and thus contribute to the inverse $\eta_{\text{vib,low}}$ observed.⁸ If the terminal methyl group in $\text{F}^-(\text{HOCH}_3)$ similarly interacts with the CH_3X methyl internal rotation at the $\text{S}_{\text{N}}2$ transition state (Figure 1B), then we can speculate that ν_{18} -type vibrational modes could account for the KIE observed for $\text{F}^-(\text{methanol}) + \text{CH}_3\text{X}$ upon the deuteration of CH_3OH to CD_3OH (or CH_3OD to CD_3OD). High-level theoretical predictions would be challenging for the subtle KIE involving the larger and floppier $\text{S}_{\text{N}}2$ transition states with a fluorine atom and are beyond the scope of this paper.

In conclusion, measured inverse deuterium KIEs are consistent with the previous results on the water-solvated $\text{S}_{\text{N}}2$ reactions. KIEs from differently labeled solvents suggest that the transition states have structures analogous to that for $\text{F}^-(\text{H}_2\text{O}) + \text{CH}_3\text{X}$. Site-specific deuteration effects have also been observed for ion–molecule association kinetics of hydroxide and alkoxide ions.²⁵ Detailed analysis of the KIEs as well as product branching will be discussed in a future publication.²⁶

Acknowledgment. This work was supported by a grant (CHE-0349937) from the National Science Foundation. On the occasion of his landmark birthday, we are pleased to dedicate this paper to Tomas Baer, a great scientist, colleague, and friend.

References and Notes

- (1) Laerdahl, J. K.; Uggerud, E. *Int. J. Mass Spectrom.* **2002**, *214*, 277.
- (2) (a) Viggiano, A. A.; Arnold, S. T.; Morris, R. A. *Int. Rev. Phys. Chem.* **1998**, *17*, 147. (b) Takashima, K.; Riveros, J. M. *Mass Spectrom. Rev.* **1998**, *17*, 409.
- (3) Bohme, D. K.; Raksit, A. B. *Can. J. Chem.* **1985**, *63*, 3007.
- (4) Seeley, J. V.; Morris, R. A.; Viggiano, A. A. *J. Phys. Chem. A* **1997**, *101*, 4598.
- (5) O'Hair, R. A. J.; Davico, G. E.; Hacialoglu, J.; Dang, T. T.; DePuy, C. H.; Bierbaum, V. M. *J. Am. Chem. Soc.* **1994**, *116*, 3609.
- (6) Tachikawa, H. *J. Phys. Chem. A* **2001**, *105*, 1260.
- (7) Poirier, R. A.; Wang, Y.; Westaway, K. C. *J. Am. Chem. Soc.* **1994**, *116*, 2526.
- (8) Hu, W.-P.; Truhlar, D. G. *J. Am. Chem. Soc.* **1994**, *116*, 7797.
- (9) Most product channels (analogous to eqs 1a and 1b) are exothermic for these reactions. The reaction enthalpies (in kcal mol^{-1}) are –8.6 ($\text{Br}^- + \text{CH}_3\text{F} + \text{CH}_3\text{OH}$), –23.1 ($\text{Br}^- (\text{CH}_3\text{OH}) + \text{CH}_3\text{F}$), –14.4 ($\text{I}^- + \text{CH}_3\text{F} + \text{CH}_3\text{OH}$), –26.3 ($\text{I}^- (\text{CH}_3\text{OH}) + \text{CH}_3\text{F}$), –11.4 ($\text{I}^- + \text{CH}_3\text{F} + i\text{-C}_3\text{H}_7\text{OH}$), –24.5 ($\text{I}^- (i\text{-C}_3\text{H}_7\text{OH}) + \text{CH}_3\text{F}$), +0.8 ($\text{I}^- + \text{CH}_3\text{F} + \text{HF}$), and –14.1 ($\text{I}^- (\text{HF}) + \text{CH}_3\text{F}$).
- (10) (a) Van Doren, J. M.; Barlow, S. E.; DePuy, C. H.; Bierbaum, V. M. *Int. J. Mass Spectrom. Ion Processes* **1987**, *81*, 85. (b) Bierbaum, V. M. *Encycl. Mass Spectrom.* **2003**, *1*, 98.
- (11) Kawaguchi, K.; Hirota, E. *J. Chem. Phys.* **1987**, *87*, 6838.
- (12) Bogdanov, B.; McMahon, T. B. *J. Phys. Chem. A* **2000**, *104*, 7871.
- (13) Baer, T.; Hase, W. L. *Unimolecular Reaction Dynamics*; Oxford University Press: New York, 1996.
- (14) Kato, S.; Davico, G. E.; Lee, H. S.; DePuy, C. H.; Bierbaum, V. M. *Int. J. Mass Spectrom.* **2001**, *210/211*, 223.
- (15) Su, T.; Chesnavich, W. J. *J. Chem. Phys.* **1982**, *76*, 5183.
- (16) *CRC Handbook of Chemistry and Physics*, 75th ed.; Lide, D. R., Ed.; CRC Press: Boca Raton, FL, 1994.
- (17) Robinson, P. J.; Holbrook, K. A. *Unimolecular Reactions*; Wiley: New York, 1972.
- (18) Davico, G. E.; Bierbaum, V. M. *J. Am. Chem. Soc.* **2000**, *122*, 1740.
- (19) Herzberg, G. *Molecular Spectra and Molecular Structure. III. Electronic Spectra and Electronic Structure of Polyatomic Molecules*; Van Nostrand Reinhold: New York, 1966.
- (20) Combariza, J. E.; Kestner, N. R. *J. Phys. Chem.* **1994**, *98*, 3513.
- (21) Herzberg, G. *Molecular Spectra and Molecular Structure. I. Spectra of Diatomic Molecules*; Van Nostrand Reinhold: New York, 1950.
- (22) Unless otherwise specified, all thermochemical values have been taken or derived from the NIST Chemistry Webbook, NIST Standard Reference Database Number 69, March 2003 release and references therein.
- (23) Bogdanov, B.; Peschke, M.; Tonner, D. S.; Szulejko, J. E.; McMahon, T. B. *Int. J. Mass Spectrom.* **1999**, *185/186/187*, 707.
- (24) Weis, P.; Kemper, P. R.; Bowers, M. T.; Xantheas, S. S. *J. Am. Chem. Soc.* **1999**, *121*, 3531.
- (25) Kato, S.; Dang, T. T.; Barlow, S. E.; DePuy, C. H.; Bierbaum, V. M. *Int. J. Mass Spectrom.* **2000**, *195/196*, 625.
- (26) Davico, G. E.; et al., to be submitted for publication.